Journal of Geophysical Research: Atmospheres

Supporting Information for

Isoprene emissions and impacts over an ecological transition region in the US Upper Midwest inferred from tall tower measurements

Lu Hu [1, 2], Dylan B. Millet [1], Munkhbayar Baasandorj [1], TimothyJ. Griffis [1], Peter Turner [1], Detlev Helmig [3], Abigale J. Curtis [3], Jacques Hueber [3]

1 University of Minnesota, St. Paul, Minnesota, USA

2 Harvard University, Cambridge, Massachusetts, USA

3 University of Colorado, Boulder, Colorado, USA

Contents of this file

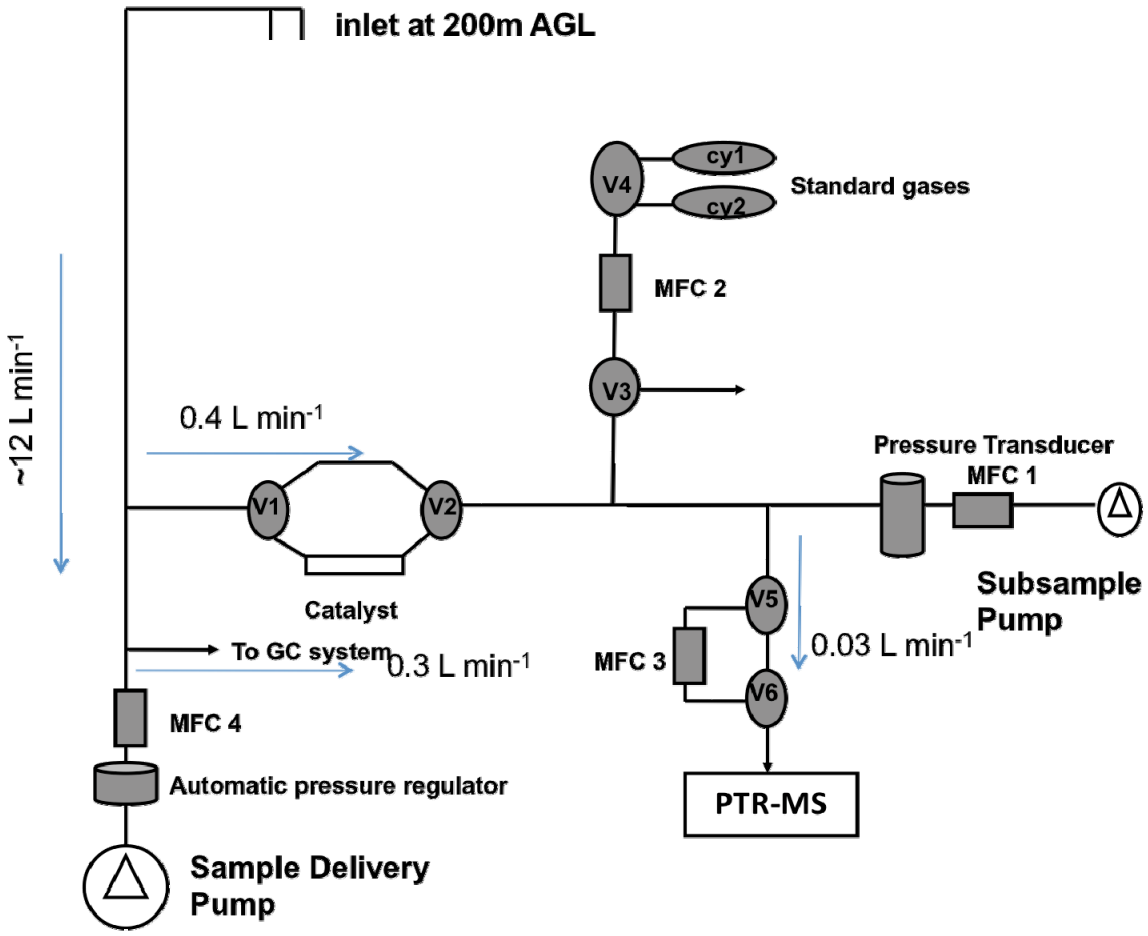

Figure S1. Schematic of the PTR-MS inlet/calibration system employed at the KCMP tall tower. MFC 1 - MFC 4: mass flow controllers 1-4; V1-V6: 3-way valves 1-6; cy1- cy2: VOC standard gases; GC System: gas chromatography with a reducing compound photometer (Peak Performer 1; Peak Laboratories LLC, USA) for measuring CO and H_2 (*Hu et al.*, 2011; *Kim et al.*, 2013); AGL: above ground level. Blue arrows show the flow directions with typical flow rates indicated.

Parameter	Value	Comments
PC (mbar)	355	Reaction chamber pressure
FC (sccm)	6.5	Water flow
U SO (V)	75	Voltage of source out to optimize the O_2 and H_3O^+ ratio
U S (V)	110	Voltage of source to optimize the O_2 and H_3O^+ ratio
U Drift (V)	600	Drift tube voltage
U QL (V)	50	Voltage of the extraction lens at the end of the reaction chamber
U NC (V)	6	Nose cone voltage
Source (mA)	6.5-8.0	Water source current
T drift (°C)	60	Drift tube temperature
T inlet (°C)	60	Inlet temperature
Rea (mbar)	2.1-2.3	Reaction chamber pressure
T catalyst (°C)	450	Temperature of the catalytic converter
Subsampling pressure (torr)	530-570	Pressure transducer in Figure S1
Main sampling line pressure (hPa)	~900	Automatic pressure regulator in Figure S1
Subsampling flow (sccm)	250-500	MFC 1 in Figure S1
Main sampling flow (L min^{-1})	~12	MFC 4 in Figure S1

Table S1. Typical PTR-MS and sampling system settings

Compound	Protonated m/z	Dwell time (s)	Sensitivity (ncps/ppbv)[a]	Sensitivity variability (%)[b]	Detection Limit (pptv)[c]	Humidity factor X_R [d]
methanol	33	5	11	<2	203	0.38
acetone	59	10	18	<4	28	0.58
isoprene	69	10	7	<9	38	0.5
MVK+MACR	71	10	8 [e]	<6	21	0.5
MEK[f]	73	10	15	<3	30	0.5
benzene	79	10	10	<6	17	-0.2
toluene	93	10	13	<9	20	0.1
C_8 aromatics	107	10	8	<2	30	0.1
C_9 aromatics	121	20	7	<5	45	0.1

[a] Sensitivities are from measurements during July 20, 2011-August 08, 2011; [b] percentage differences between the highest and lowest sensitivity during July 20, 2011-August 08, 2011 ((high/low-1)*100%); [c] Detection limits are defined as 3 times the error in the volume mixing ratios, following Equation (2.17) of *de Gouw and Warneke* (2007); [d] X_R values to correct the measurements for the influence of humidity, are from Table 1 of *de Gouw et al.* (2003); [e] subject to MVK and MACR loss in the pre-mixed VOC standard cylinders as described in Section 2.2; [f] Methyl Ethyl Ketone.

Table S2. Figures of merit for selected compounds measured at the KCMP tall tower

Sensitivity runs	Notes
Base	Simulation using CLM4 vegetation, with the model values taken as an inverse distance-weighted mean of the 4-intersecting grid cells as described in Section 5.
NASS	Same as *Base* except using USDA NASS land cover for the region surrounding the KCMP tall tower.
Br	Same as *Base*, except including bromine chemistry, which modifies the model oxidant fields [*Parrella et al.*, 2012].
HO_2	Same as *Base*, except using a reactive uptake coefficient for HO_2 on aqueous aerosols of 0.4 rather than 0.2 [*Mao et al.*, 2013].
Alt. chemistry	Same as *Base*, except using a previous model representation of isoprene chemistry [*Palmer et al.*, 2006; *Millet et al.*, 2008].
PBL	Same as *Base*, except using a local rather than a non-local scheme for boundary layer mixing in the model [*Lin and McElroy*, 2010].
$DryDep_{f0=0}$	Same as *Base*, except using a coefficient for reactive uptake of MVK and MACR by vegetation of 0 rather than 1.
$K_{RO2+HO2}$	Same as *Base*, except using an updated rate of reaction for >C2 RO_2 radicals with HO_2. For the *Base* simulation: k = 7.40E-13*EXP(700/T) For this $K_{RO2+HO2}$ simulation: k = 2.91E-13*EXP(1300/T)[1-EXP(-0.245*n)], where n = # of carbon atoms. [see http://wiki.seas.harvard.edu/geos-

	chem/index.php/New_isoprene_scheme#Update_One_-_RO2.2BHO2_Reaction_Rate]
$Enox_{distribution}$	Same as *Base*, except with redistributed NO_x emissions. Here, NO_x emissions in the grid box northeast of the tower location (second grid box from the top and from the left in Fig. 2) are set equal to those in its adjacent boxes to the north and east (~0.05e12 molec/cm^2/s), and the residual emissions added to the grid box containing the Twin Cities downtowns (i.e., the grid box immediately northward of the tower location, ~0.2e12 + 0.30e12 molec/cm^2/s).
ISOPOOH	Same as *Base*, except the modeled MVK+MACR mixing ratios are replaced with the model sum of MVK+MACR+ISOPOOH+0.3*IEPOX to test how the potential detection of isoprene hydroperoxides (ISOPOOH) and isoprene epoxydiols (IEPOX) as MVK+MACR in the PTR-MS might influence the model-measurement comparisons [*Liu et al.*, 2013; *Rivera-Rios et al.*, 2014].
Combined	Combines the following 4 sensitivity analyses: $DryDep_{f0=0}$, $K_{RO2+HO2}$, $Enox_{distribution}$, and *ISOPOOH*.
*Eisop*x.x*	Same as *Base*, except isoprene emissions are multiplied by a factor of x.x
*Enox*x.x*	Same as *Base*, except NO_x emissions are multiplied by a factor of x.x

Table S3. Description of sensitivity simulations presented in Figure 10

References:

de Gouw, J. A., C. Warneke, T. Karl, G. Eerdekens, C. van der Veen, and R. Fall (2003), Sensitivity and specificity of atmospheric trace gas detection by proton-transfer-reaction mass spectrometry, *Int. J. Mass Spectrom.*, *223*(1-3), 365-382, doi:10.1016/S1387-3806(02)00926-0

de Gouw, J. A., and C. Warneke (2007), Measurements of volatile organic compounds in the earth's atmosphere using proton-transfer-reaction mass spectrometry, *Mass Spectrom. Rev.*, *26*(2), 223-257, doi:10.1002/mas.20119.

Hu, L., D. B. Millet, M. J. Mohr, K. C. Wells, T. J. Griffis, and D. Helmig (2011), Sources and seasonality of atmospheric methanol based on tall tower measurements in the US Upper Midwest, *Atmos. Chem. Phys.*, *11*(21), 11145-11156, doi:10.5194/acp-11-11145-2011.

Lin, J. T., and M. B. McElroy (2010), Impacts of boundary layer mixing on pollutant vertical profiles in the lower troposphere: Implications to satellite remote sensing, *Atmos. Environ.*, *44*(14), 1726-1739, doi:10.1016/j.atmosenv.2010.02.009.

Liu, Y. J., I. Herdlinger-Blatt, K. A. McKinney, and S. T. Martin (2013), Production of methyl vinyl ketone and methacrolein via the hydroperoxyl pathway of isoprene oxidation, *Atmos. Chem. Phys.*, *13*(11), 5715-5730, doi:10.5194/acp-13-5715-2013.

Kim, S. Y., D. B. Millet, L. Hu, M. J. Mohr, T. J. Griffis, D. Wen, J. C. Lin, S. M. Miller, and M. Longo (2013), Constraints on carbon monoxide emissions based on tall tower measurements in the U.S. Upper Midwest, *Environ. Sci. Technol.*, *47*(15), 8316-8324, doi:10.1021/es4009486.

Mao, J., D. J. Jacob, M. J. Evans, J. R. Olson, X. Ren, W. H. Brune, J. M. S. Clair, J. D. Crounse, K. M. Spencer, M. R. Beaver, P. O. Wennberg, M. J. Cubison, J. L. Jimenez, A. Fried, P. Weibring, J. G. Walega, S. R. Hall, A. J. Weinheimer, R. C. Cohen, G. Chen, J. H. Crawford, C. McNaughton, A. D. Clarke, L. Jaeglé, J. A. Fisher, R. M. Yantosca, P. Le Sager, and C. Carouge (2010), Chemistry of hydrogen oxide radicals (HO_x) in the Arctic troposphere in spring, *Atmos. Chem. Phys.*, *10*(13), 5823-5838, doi:10.5194/acp-10-5823-2010.

Millet, D. B., D. J. Jacob, K. F. Boersma, T.-M. Fu, T. P. Kurosu, K. Chance, C. L. Heald, and A. Guenther (2008), Spatial distribution of isoprene emissions from North America derived from formaldehyde column measurements by the OMI satellite sensor, *J. Geophys. Res.*, *113*(D2), D02307, doi:10.1029/2007jd008950.

Palmer, P. I., D. S. Abbot, T.-M. Fu, D. J. Jacob, K. Chance, T. P. Kurosu, A. Guenther, C. Wiedinmyer, J. C. Stanton, M. J. Pilling, S. N. Pressley, B. Lamb, and A. L. Sumner (2006), Quantifying the seasonal and interannual variability of North American isoprene emissions using satellite observations of the formaldehyde column, *J. Geophys. Res.*, *111*(D12), D12315, doi:10.1029/2005jd006689.

Parrella, J. P., D. J. Jacob, Q. Liang, Y. Zhang, L. J. Mickley, B. Miller, M. J. Evans, X. Yang, J. A. Pyle, N. Theys, and M. Van Roozendael (2012), Tropospheric bromine chemistry: implications for present and pre-industrial ozone and mercury, *Atmos. Chem. Phys.*, *12*(15), 6723-6740, doi:10.5194/acp-12-6723-2012.

Rivera-Rios, J. C., T. B. Nguyen, J. D. Crounse, W. Jud, J. M. St. Clair, T. Mikoviny, J. B. Gilman, B. M. Lerner, J. B. Kaiser, J. de Gouw, A. Wisthaler, A. Hansel, P. O. Wennberg, J. H. Seinfeld, and F. N. Keutsch (2014), Conversion of hydroperoxides to carbonyls in field and laboratory instrumentation: observational bias in diagnosing pristine versus anthropogenically-controlled atmospheric chemistry, *Geophys. Res. Lett.*, 2014GL061919, 10.1002/2014gl061919.